ORNL/TM-5331

Theoretical and Experimental Determination of Mechanical Properties of Superconducting Composite Wire

W. H. Gray
C. T. Sun

AMPTIAC

MASTER

OAK RIDGE NATIONAL LABORATORY
OPERATED BY UNION CARBIDE CORPORATION FOR THE ENERGY RESEARCH AND DEVELOPMENT ADMINISTRATION

Printed in the United States of America. Available from
National Technical Information Service
U.S. Department of Commerce
5285 Port Royal Road, Springfield, Virginia 22161
Price: Printed Copy ~~$4.50~~; Microfiche ~~$2.25~~

ORNL/TM-5331

Contract No. W-7405-eng-26

THEORETICAL AND EXPERIMENTAL DETERMINATION OF MECHANICAL PROPERTIES OF SUPERCONDUCTING COMPOSITE WIRE

W. H. Gray
Superconducting Magnet Development Program
Thermonuclear Division

and

C. T. Sun
Iowa State University

JULY 1976

OAK RIDGE NATIONAL LABORATORY
Oak Ridge, Tennessee 37830
operated by
UNION CARBIDE CORPORATION
for the
ENERGY RESEARCH AND DEVELOPMENT ADMINISTRATION

TABLE OF CONTENTS

THEORETICAL AND EXPERIMENTAL DETERMINATION OF MECHANICAL PROPERTIES OF SUPERCONDUCTING COMPOSITE WIRE*

W. H. Gray and C. T. Sun†

ABSTRACT

The object of this research is to characterize the mechanical properties of a composite superconducting (NbTi/Cu) wire in terms of the mechanical properties of each constituent material. For a particular composite superconducting wire, five elastic material constants were experimentally determined and theoretically calculated.

Since the Poisson's ratios for the fiber and the matrix material were very close, there was essentially no (less than 1%) difference among all the theoretical predictions for any individual mechanical constant. Because of the expense and difficulty of producing elastic constant data of 0.1% accuracy, and therefore conclusively determining which theory is best, no further experiments were performed.

INTRODUCTION

The object of this research is to characterize the mechanical properties of a composite superconducting (NbTi/Cu) wire in terms of the mechanical properties of each constituent material. In 1973, the Cryogenics Division of the National Bureau of Standards (NBS) published an interim report[1] in which a preliminary investigation of the mechanical properties of a solenoid coil composite was made. The coil investigated consisted of epoxy, fiberglass, and composite superconducting wire. Both theoretical and experimental elastic constants were tabulated

---

* This research was sponsored in part by the Engineering Research Institute, Iowa State University, Ames, IA 50011, and in part by the Energy Research and Development Administration under contract with Union Carbide Corporation.

† Department of Engineering Sciences and Mechanics and Engineering Research Institute, Iowa State University, Ames, IA 50011.

for a typical piece of coil cut out of a small solenoid. Our report differs from this NBS work in that we consider only the mechanical properties of an individual composite superconducting wire.

The theoretical predictions and the experimental procedures to determine the effective elastic constants of the composite wire are described in the next two sections of this report.

THEORETICAL INVESTIGATION

Most of the analytical work for predicting the mechanical and thermal properties of fiber-reinforced composites in terms of volumetric composition, geometrical arrangement of the fibers, and constituent material properties was done before 1970. There are five approaches to predict the micromechanical behavior of fiber-reinforced composites.* The essential characteristic of each is described below.

1.1 SELF-CONSISTENT MODEL METHODS

This method was originally proposed by Hershey[3] and Kroner[4] for crystal aggregates, and was first employed by Hill[5] to derive expressions for elastic constants. Hill modeled the composite as a single fiber embedded in an unbounded macroscopically homogeneous medium, subjected to a uniform loading at infinity. This uniform loading produces a uniform strain field in the filament which is then used to estimate the elastic constants. A similar model proposed by Frohlich and Sack[6] for predicting the viscosity of a Newtonian fluid containing a dispersion of equal elastic spheres consists of three concentric cylinders, the outer one being unbounded. The innermost cylinder is assumed to have the elastic properties of the filaments; the middle one has the properties of the matrix; and the outermost has the properties of the composite. The solid is subjected to homogeneous stresses at infinity. The resulting elastic fields are determined, and then are

* No attempt is made here to give a comprehensive literature survey regarding this subject. More references can be found in Ref. 2.

employed to predict the elastic constants of the composite. Applications of the self-consistent model methods can be found, for example, in Refs. 7-9.

1.2 VARIATIONAL METHODS

In this method, the energy theorems of classical elasticity are used to obtain bounds on the mechanical and physical properties of filamentary composites. The minimum complementary energy theorem yields a lower bound, while the minimum potential energy theorem yields the upper bound. Using this approach, bounds for the elastic and thermal properties of composites have been obtained by many investigators.[10-12]

1.3 EXACT METHODS

By assuming that the fibers are arranged in a doubly periodic rectangular array, a fundamental or repeating element can be established. The resulting elasticity problem can then be solved either by introducing a stress function using a series development, or by numerical techniques such as finite difference or finite element methods. Once the problem is solved elastically, the resulting elastic fields can be averaged to get expressions for the desired elastic constants. Typical applications of this method can be found in Refs. 13-18.

1.4 MECHANICS OF MATERIALS METHOD

By making simplifying assumptions regarding the mechanical or thermal behavior of a composite material, the mechanics-of-materials expressions for the equivalent elastic or thermal constants of unidirectionally reinforced fibrous composite materials can be derived. For example, to determine the longitudinal Young's modulus, one assumes that the longitudinal strains in both the matrix and the fiber are the same; in order to determine the transverse Young's modulus, one assumes that transverse stresses in both materials are the same. This approach

usually is referred to as the "rule of mixtures." The "rule of mixtures" expressions for elastic moduli and thermal conductivities can be found in Refs. 19-21.

1.5 THE HALPIN-TSAI EQUATIONS

For designers, it is often necessary to have simple and rapid computational procedures for estimating the macromechanical properties of a fibrous composite. Such empirical formulas have been developed by Halpin and Tsai[22] based upon modifications of the results discussed under approaches 1.1 and 1.3. By estimating the value of a factor which depends on the geometry of the inclusions, spacing geometry, and loading conditions, the composite elastic moduli can be approximated. Reliable estimates for this factor can be obtained by comparing the Halpin-Tsai equation with the numerical micromechanics solutions. If used appropriately, the Halpin-Tsai equation can yield very reliable results without elaborate calculations.

All the above methods make the following three basic assumptions: (1) each constituent material behaves linearly elastically, (2) the fibers are straight (without twist), and (3) there are no residual stresses. For this investigation, we use several of the available theoretical equations to predict the effective elastic mechanical properties of superconducting composite wire. These equations are listed in Appendix I.

In general, a superconducting composite wire may be twisted to minimize ac power losses in a superconducting magnet. Twisting of the wire violates an assumption implicit in the derivation of all the equations presented in Appendix I. However, we believe that this effect is small (see Appendix II), and for engineering purposes can be neglected. Other effects, such as inelastic behavior of the wire at higher loading levels, and residual stresses in the wire introduced during fabrication, may influence the results presented in this paper, and should be analyzed more thoroughly.

EXPERIMENTAL DETERMINATION OF ELASTIC CONSTANTS

Assuming the NbTi/Cu wire behaves like a transversely isotropic material, there are five elastic constants of significance. These constants are: (1) Young's modulus along the direction of the fiber, E_L or E_{11} (longitudinal Young's modulus), (2) major Poisson's ratio, ν_L or ν_{12}, (3) Young's modulus along the direction normal to the fiber, E_T or E_{22} (transverse Young's modulus), (4) minor Poisson's ratio, ν_T or ν_{23}, and (5) longitudinal shear modulus, G_L or G_{12}. Since the material properties in a plane normal to the fiber direction are assumed to be isotropic, the transverse shear modulus G_T or G_{23} can be determined from the isotropic relation

$$G_T = \frac{E_T}{2(1 + \nu_T)} \qquad (1)$$

The particular superconducting composite wire chosen for our experiment was KRYO-210.*†[23] This conductor has cross-sectional dimensions of 10.16 mm by 5.08 mm with a copper matrix containing 2640 Nb-45 wt % Ti superconducting filaments. The copper to superconductor ratio is 6. The elastic constants which were used for the comparisons are tabulated below. All elastic constant measurements were made at room temperature.

Material	Young's Modulus (GPa)	Poisson's Ratio	Shear Modulus (GPa)
Cu	123	0.345	45.7
NbTi	84	0.33	31.5

* Registered trademark of Magnetics Corporation of America (MCA).

† Tradenames of material are used in this report for clarity. In no case does such selection imply recommendations or endorsement by the authors, nor does it imply that the material is necessarily the best available for the purpose.

2.1 EXPERIMENTAL DETERMINATION OF E_{11} AND ν_{12}

E_{11} and ν_{12} can be determined from a simple tension test (see Fig. 1). The direction of loading is parallel to the fibers of the conductor. The longitudinal Young's modulus is determined from a σ_1 vs ε_1 diagram where σ_1 is equal to the applied load divided by the cross sectional area of the specimen, and ε_1 is the strain along the fiber direction of the conductor. Figure 2 represents an experimentally determined plot of this diagram for KRYO-210 superconductor showing a value for E_{11} of 119 GPa. A comparison of the theoretical prediction and the experimental data is shown in Fig. 3 in this graph, as well as the four normalized comparison graphs which follow; the legend refers to the theoretical equations presented in Appendix I. Both equations predict the same behavior, which deviates approximately 3% from the experimental data.

The major Poisson's ratio is determined from the slope of the ε_2 vs ε_1 diagram during the same experiment, where ε_2 is the strain in either transverse direction. The experimentally determined value was 0.347 (see Fig. 4). The normalized plot (see Fig. 5) showing the comparison between theoretical prediction and experimental value again demonstrates little difference between theories with the experimental data differing from the predictions by about 2%.

2.2 EXPERIMENTAL DETERMINATION OF E_{22} AND G_{23}

E_{22} and G_{23} are determined from a test similar to that described in 2.1 (see Fig. 6). The direction of the applied load is normal to the fiber axis. The transverse Young's modulus is determined from the σ_2 vs ε_2 diagram where σ_2 is the stress, and ε_2 is the strain in the direction of the applied force. Figure 7 represents an experimentally determined plot of this diagram for KRYO-210 superconductor showing a value for E_{22} of 122 GPa. The experimental data are compared to the theoretical predictions for E_{22} in Figure 8. An error of approximately 5% is observed.

Analogously the minor Poisson's ratio, and therefore G_{23}, is determined from an ε_3 vs ε_2 diagram. The experimental value for G_{23} is 43.1 GPa (see Fig. 9). Figure 10 compares this data point with the

theoretical predictions. An error of approximately 2% is observed.

2.3 EXPERIMENTAL DETERMINATION OF THE LONGITUDINAL SHEAR MODULUS G_{12}

The simplest way to determine the longitudinal shear modulus G_{12} is to use a tensile specimen with the fibers oriented at a 45^o direction to the geometrical axis of the specimen.[24] A realistic specimen of a composite superconductor, however, would be very difficult and expensive to fabricate. An alternate method to evaluate G_{12} experimentally is outlined below.

From the two-dimensional anisotropic stress-strain relation, we have

$$\begin{Bmatrix} \varepsilon_\Theta \\ \varepsilon_{\Theta+\pi/2} \\ \gamma_\Theta \end{Bmatrix} = \begin{bmatrix} \bar{S}_{11} & \bar{S}_{12} & \bar{S}_{16} \\ \bar{S}_{12} & \bar{S}_{22} & \bar{S}_{26} \\ \bar{S}_{16} & \bar{S}_{26} & \bar{S}_{66} \end{bmatrix} \begin{Bmatrix} \sigma_\Theta \\ \sigma_\Theta \\ \tau_\Theta \end{Bmatrix} \quad (2)$$

where ε_Θ and $\varepsilon_{\Theta + \pi/2}$ are the axial strains of x' and z' axes. These lie in the xz plane and make angles θ and $\theta + \pi/2$ with the x-axis respectively; γ_θ is the shear strain of x' and z' axes, and σ_θ, $\sigma_{\theta + \pi/2}$ and τ_θ are the corresponding normal and shear stresses respectively (see Figure 11). The matrix $[\bar{S}]$ in Eq. (2) represents the compliance matrix of the composite material in x'z' directions. In a simple tension test with the applied load and the fibers oriented along the x direction, ε_θ and $\varepsilon_{\theta + \pi/2}$ can be measured directly and γ_θ can be computed, using the data obtained from strain gage rosette readings. For axial tension, σ_θ, $\sigma_{\theta + \pi/2}$ and τ_θ are given by

$$\begin{aligned} \sigma_\Theta &= \sigma_x \cos^2\Theta \\ \sigma_{\Theta+\pi/2} &= \sigma_x \sin^2\Theta \\ \tau_\Theta &= -\sigma_x \sin\Theta\cos\Theta \end{aligned} \quad (3)$$

where σ_x is equal to the applied force divided by the cross sectional area of the specimen. The elastic compliances $\bar{S}_{11}$, $\bar{S}_{12}$, $\bar{S}_{22}$, $\bar{S}_{16}$, $\bar{S}_{26}$, and $\bar{S}_{66}$ are related to E_{11}, E_{22}, ν_{12}, and G_{12} by the following relations.[2]

$$\bar{S}_{11} = \frac{\cos^4\Theta}{E_{11}} + 2\left(\frac{1}{G_{12}} - \frac{\nu_{12}}{E_{11}}\right)\sin^2\Theta\cos^2\Theta + \frac{\sin^4\Theta}{E_{22}} \quad (4)$$

$$\bar{S}_{12} = \left(\frac{1}{E_{11}} + \frac{1}{E_{22}} - \frac{2}{G_{12}}\right)\sin^2\Theta\cos^2\Theta - \frac{\nu_{12}}{E_{11}}(\sin^4\Theta + \cos^4\Theta) \quad (5)$$

$$\bar{S}_{22} = \frac{\sin^4\Theta}{E_{11}} + 2\left(\frac{1}{G_{12}} - \frac{\nu_{12}}{E_{11}}\right)\sin^2\Theta\cos^2\Theta + \frac{\cos^4\Theta}{E_{22}} \quad (6)$$

$$\bar{S}_{16} = \left(\frac{1}{E_{11}} + \frac{\nu_{12}}{E_{11}} - \frac{1}{G_{12}}\right)\sin\Theta\cos^3\Theta + \left(\frac{1}{G_{12}} - \frac{\nu_{12}}{E_{11}} - \frac{1}{E_{22}}\right)\sin^3\Theta\cos\Theta \quad (7)$$

$$\bar{S}_{26} = \left(\frac{1}{E_{11}} + \frac{\nu_{12}}{E_{11}} - \frac{1}{G_{12}}\right)\sin^3\Theta\cos\Theta + \left(\frac{1}{G_{12}} - \frac{\nu_{12}}{E_{11}} - \frac{1}{E_{22}}\right)\sin\Theta\cos^3\Theta \quad (8)$$

$$\bar{S}_{66} = \left(\frac{1}{E_{11}} + \frac{1}{E_{22}} + \frac{2\nu_{12}}{E_{11}} - \frac{1}{G_{12}}\right)\sin^2\Theta\cos^2\Theta + \frac{1}{2G_{12}}(\sin^4\Theta + \cos^4\Theta) \quad (9)$$

Since E_{11}, E_{22}, and ν_{12} are determined from tests (2.1) and (2.2), and ϵ_θ, $\epsilon_{\theta+\pi/2}$, γ_θ, σ_θ, $\sigma_{\theta+\pi/2}$, and τ_θ are obtained either from direct measurement by strain gages or from Eq. (3), the only unknown in Eq. (2) is G_{12}. Thus G_{12} can be computed from any one of the three equations in Eq. (2). Its value is found to be 44.8 GPa which is within 5% of the theoretical predictions (see Fig. 12).

CONCLUSIONS

The goal of this experiment was to determine which theory of composites best predicted the elastic mechanical behavior of a superconducting (NbTi/Cu) composite wire. Examination of each elastic mechanical property reveals that all theories examined are capable of predicting experimental data to within 5%.

Since the Poisson's ratios for both the fiber and the matrix material were very close, there was essentially no (less than 1%) difference among all the theoretical predictions for any individual mechanical constant. Because of the expense and difficulty of producing elastic constant data within 0.1% accuracy, and therefore, conclusively determining which theory is best, no further experiments were performed.

In conclusion, for a superconducting composite wire, NbTi/Cu, a simple, fast, and reliable engineering estimate of its elastic mechanical behavior can be made by using the "rule of mixtures." It is unnecessary to use one of the more rigorous theories.

REFERENCES

1. C. W. Fowlkes et al., "Characterization of a Superconducting Coil Composite," NBSIR-73-349, Boulder, Colorado (1973).

2. J. E. Ashton, J. C. Halpin, and P. H. Petit, Primer on Composite Materials: Analysis, Technomic Publishing Co., Stamford, Connecticut (1969).

3. A. V. Hershey, "The Elasticity of an Isotropic Aggregate of Anisotropic Cubic Crystals," J. of Appl. Mech. 21, 235 (1954).

4. E. Kroner, "Berechnung der Elastischen Konstanten des Vielkristalls aus den Konstanten des Einkristalls," Z. Phys. 151, 504 (1958).

5. R. Hill, "Theory of Mechanical Properties of Fiber-strengthened Materials Self-consistent Model," Journal of Mechanics and Physics of Solids 13, 189 (1965).

6. H. Frohlich and B. Sack, "Theory of the Rheological Properties of Dispersion," Proc. R. Soc. Lond. A185, 415 (1946).

7. J. J. Hermann, "The Elastic Properties of Fiber Reinforced Materials When the Fibers are Aligned," Proceedings Koninklijke Nederlands Akademic van Westenschappen, Amsterdam Series 3. 70(1), 1 (1967).

8. Z. Hashin, "Assessment of the Self-consistent Scheme Approximation - Conductivity of Particulate Composites," Journal of Composite Materials 2, 284 (1968).

9. Z. Hashin and W. Rosen, "The Elastic Moduli of Fiber-Reinforced Materials," J. of Appl. Mech. 31, 223 (1964).

10. Z. Hashin, "On Elastic Behavior of Fiber-Reinforced Materials of Arbitrary Transverse Phase Geometry," Journal of Mechanics and Physics of Solids 13, 119 (1965).

11. R. A. Schapery, "Thermal Expansion Coefficients of Composite Materials Based on Energy Principle," Journal of Composite Materials 2(3), 380 (1968).

12. R. Hill, "Theory of Mechanical Properties of Fiber-Strengthened Materials: Elastic Behavior," Journal of Mechanical Physics of Solids 2, 199 (1964).

13. D. F. Adams and D. R. Doner, "Longitudinal Shear Loading of a Unidirectional Composite," Journal of Composite Materials 1, 152 (1967).

14. D. F. Adams and D. R. Doner, "Transverse Normal Loading of a Unidirectional Composite," Journal of Composite Materials 1, 152 (1967).

15. C. H. Chen and S. Cheng, "Mechanical Properties of Fiber-Reinforced Composites," Journal of Composite Materials 1, 30 (1967).

16. E. Behrens, "Thermal Conductivity of Composite Materials," Journal of Composite Materials 2(1), 2 (1968).

17. S. I. Kang and G. M. Rentzepis, "On the Determination of Physical Properties of Composite Materials by a Three-Dimensional Finite Element Procedure," Composite Materials: Testing and Design, American Society for Testing and Materials Special Technical Publication S46, Philadelphia, Pennsylvania (1973).

18. R. M. Barker, F. T. Lin and J. R. Dana, "Three-Dimensional Finite-Element Analysis of Laminated Composites," Computers and Structures 2, 1013-1029 (1972).

19. R. M. Jones, Mechanics of Composite Materials, McGraw-Hill, New York (1974).

20. J. C. Ekvall, "Elastic Properties of Orthotropic Monofilament Laminates," paper 61-AV56 presented at American Society of Mechanical Engineers Aviation Conference, Los Angeles, California (March 1961).

21. G. S. Springer and S. W. Tsai, "Thermal Conductivity of Unidirectional Materials," Journal of Composite Materials 1, 166 (1967).

22. J. C. Halpin and S. W. Tsai, "Environmental Factors in Composite Materials Design," AFML-TR-67-423, Air Force Materials Laboratory, (1967).

23. G. A. Miranda and J. D. Rogers, "Adjacent Conductor Field Corrections to High Critical Current Short Sample Measurements," LA-UR-74-1413, Los Alamos, New Mexico (1974).

24. B. W. Rosen, "A Simple Procedure for Experimental Determination of the Longitudinal Shear Modulus of Unidirectional Composites," Journal of Composite Materials 6, 552 (October 1972).

25. J. M. Whitney, "Geometrical Effects of Filament Twist on the Modulus and Strength of Graphite Fiber-Reinforced Composites," Textile Research Journal 36(9), 765 (September 1966).

NOMENCLATURE

Symbol Definition

E - Young's modulus

G - Shear modulus

ν - Poisson's ratio

K - Bulk modulus in plane strain

V - Volume fraction

f - Fiber material (NbTi)

m - Matrix material (Cu)

L - Composite material constants along the fiber direction

T - Composite material constants along a transverse direction

APPENDIX I

This appendix presents the various theoretical equations which were used to predict the elastic mechanical properties for the superconducting composite wire studied in this report. Their alphabetic index refers to the legend on the particular graph where a comparison with experimental data was performed. Also included in this appendix is the reference in which these equations may be found.

A program which numerically tabulates all of these equations is listed in Appendix III.

1. Longitudinal Young's modulus E_L

(a) $E_L = E_m V_m + E_f V_f$ (10)

Source: Reference 2

(b) $E_L = \left(E_m V_m + E_f V_f\right) \phi$ (11)

$$\phi = \frac{E_m (D_1 - D_3 F_1) + E_f (D_2 - D_4 F_2)}{E_m (D_1 - D_3) + E_f (D_2 - D_4)}$$

$$D_1 = 1 - \nu_f \qquad D_2 = \frac{1 + V_f}{V_m} + \nu_m$$

$$D_3 = 2\nu_f^{\,2} \qquad D_4 = 2\nu_m^{\,2} \frac{V_f}{V_m}$$

$$F_1 = \frac{\nu_m V_f E_f + \nu_f V_m E_m}{\nu_f E_f V_f + V_m E_m \nu_f}$$

$$F_2 = \frac{\nu_f}{\nu_m} F_1$$

Source: Reference 10

2. Major Poisson's ratio ν_L

(a) $$\nu_L = \frac{V_f E_f L_1 + V_m E_m \nu_m L_2}{V_f E_f L_3 + V_m E_m L_2} \qquad (12)$$

$$L_1 = 2\nu_f\left(1 - \nu_m^2\right)V_f + \nu_m\left(1 + \nu_m\right)V_m$$

$$L_2 = \left(1 - \nu_f - 2\nu_f^2\right)V_f$$

$$L_3 = 2\left(1 - \nu_m^2\right)V_f + \left(1 + \nu_m\right)V_m$$

Source: Reference 10

(b) $$\nu_L = \nu_m V_m + \nu_f V_f \qquad (13)$$

Source: Reference 2

3. Transverse Young's modulus E_T

(a) $$E_T = \frac{E_f E_m}{E_f V_m + E_m V_f} \qquad (14)$$

Source: Reference 23

(b) $$E_T = \frac{1 + \phi\eta V_f}{1 - \eta V_f} E_m \qquad (15)$$

$$\eta = \frac{\frac{E_f}{E_m} - 1}{\frac{E_f}{E_m} + \phi}$$

$\phi = 2$ for circular fiber

$\phi = 2\left(\frac{a}{b}\right)$ for rectangular fiber

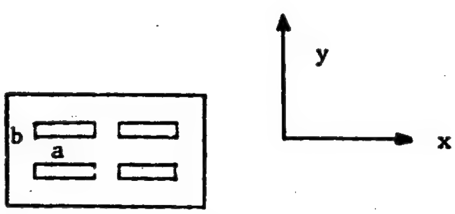

$E_T = E_x$

Source: Reference 2

(c) $E_T =$

$$2\left[1 - \nu_f + \left(\nu_f - \nu_m\right)V_m\right] \frac{M_f(2M_m + G_m) - G_m(M_f - M_m)V_m}{2M_m + G_m + 2(M_f - M_m)V_m} \qquad (16)$$

$$M_f = \frac{E_f}{2(1 - \nu_f)} \qquad M_m = \frac{E_m}{2(1 - \nu_m)}$$

Source: Reference 23

(d) $$\frac{E_T}{E_m} = \left(1 - 2\sqrt{\frac{V_f}{\pi}}\right) + \frac{1}{\alpha}\left\{\pi - \frac{4}{\sqrt{1-\frac{\alpha^2 V_f}{\pi}}}\tan^{-1}\left[\frac{\sqrt{1-(\alpha^2 V_f/\pi)}}{1+\sqrt{\alpha^2 V_f/\pi}}\right]\right\} \qquad (17)$$

$$\alpha = 2\left(\frac{E_m}{E_f} - 1\right)$$

Source: Reference 23

(e) $$\frac{1}{E_T} = \frac{V_m}{E_m} + \frac{V_f}{E_f} - \frac{V_f}{E_f}\frac{\left(\frac{E_f}{E_m}\nu_m - \nu_f\right)^2}{\frac{V_f E_f}{V_m E_m} + 1} \qquad (18)$$

Source: Reference 23

4. Transverse shear modulus G_T

(a) G_T (lower bound) $= G_m \left[1 - \frac{2(1-\nu_m)}{1-2\nu_m} V_f A_4^{\varepsilon}\right]$ (19)

where A_4^{ε} is obtained by solving the following equations

$$[P]\begin{Bmatrix} A_1 \\ A_2 \\ A_3 \\ A_4^{\varepsilon} \\ B_1 \\ B_2 \end{Bmatrix} = \begin{Bmatrix} 1 \\ 0 \\ 0 \\ 0 \\ 0 \\ 0 \end{Bmatrix}$$

where

$$[P] = \begin{bmatrix} 1 & V_f^{-1} & V_f^2 & V_f & 0 & 0 \\ 0 & \frac{1}{V_f}\cdot\frac{4\nu_m - 3}{3 - 2\nu_m} & -2V_f^2 & \frac{V_f}{1 - 2\nu_m} & 0 & 0 \\ 1 & 1 & 1 & 1 & -1 & -1 \\ 0 & \frac{4\nu_m - 3}{3 - 2\nu_m} & -2 & \frac{1}{1 - 2\nu_m} & 0 & \frac{3 - 4\nu_f}{3 - 2\nu_f} \\ 1 & \frac{3}{3 - 2\nu_m} & -3 & \frac{1}{1 - 2\nu_m} & -\frac{G_f}{G} & \frac{3\,G_f/G_m}{2\nu_f - 3} \\ 0 & -\frac{1}{3 - 2\nu_m} & 2 & \frac{-1}{1 - 2\nu_m} & 0 & \frac{G_f/G_m}{3 - 2\nu_f} \end{bmatrix}$$

Source: Reference 10

(b) $$G_T \text{ (upper bound)} = G_m \left[\frac{1}{1 + \frac{2(1 - \nu_m)}{1 - 2\nu_m} V_f A_4^\sigma} \right] \qquad (20)$$

and A_4^σ is obtained by solving

$$[R] \begin{Bmatrix} A_1 \\ A_2 \\ A_3 \\ A_4^\sigma \\ B_1 \\ B_2 \end{Bmatrix} = \begin{Bmatrix} 1 \\ 0 \\ 0 \\ 0 \\ 0 \\ 0 \end{Bmatrix}$$

where

$$[R] = \begin{bmatrix} 1 & \frac{3}{3 - 2\nu_m} \frac{1}{V_f} & -3V_f^2 & \frac{V_f}{1 - 2\nu_m} & 0 & 0 \\ 0 & \frac{-1}{3 - 2\nu_m} \frac{1}{V_f} & 2V_f^2 & \frac{-V_f}{1 - 2\nu_m} & 0 & 0 \\ 1 & 1 & 1 & 1 & -1 & -1 \\ 0 & \frac{4\nu_m - 3}{3 - 2\nu_m} & -2 & \frac{1}{1 - 2\nu_m} & 0 & \frac{3 - 4\nu_f}{3 - 2\nu_f} \\ 1 & \frac{3}{3 - 2\nu_m} & -3 & \frac{1}{1 - 2\nu_m} & -\frac{G_f}{G_m} & \frac{3\ G_f/G_m}{2\nu_f - 3} \\ 0 & -\frac{1}{3 - 2\nu_m} & 2 & \frac{-1}{1 - 2\nu_m} & 0 & \frac{G_f/G_m}{3 - 2\nu_f} \end{bmatrix}$$

Source: Reference 10

(c) $$G_T = G_m \frac{2G_f\left(K_m + G_m\right)V_f + 2G_mG_fV_m + K_mV_m\left(G_m + G_f\right)}{2G_m\left(K_m + G_m\right)V_f + 2G_mG_fV_m + K_mV_m\left(G_m + G_f\right)} \tag{21}$$

Source: Reference 7

(d) $$G_T \text{ (lower bound)} = G_m + \frac{V_f}{\frac{1}{G_f - G_m} + \frac{(K_m + 2G_m V_m)}{2G_m(K_m + G_m)}} \tag{22}$$

Source: Reference 11

(e) $$G_T \text{ (upper bound)} = G_f + \frac{V_m}{\frac{1}{G_m - G_f} + \frac{K_f + 2G_f V_f}{2G_f(K_f + G_f)}} \tag{23}$$

Source: Reference 11

5. Longitudinal shear modulus G_L

$$\text{(a)} \quad G_L = \frac{G_f\,(1 + V_f) + V_m}{\frac{G_f}{G_m} V_m + 1 + V_f} \tag{24}$$

Source: Reference 10

$$\text{(b)} \quad G_L = \frac{G_f G_m}{V_m G_f + V_f G_m} \tag{25}$$

Source: Reference 23

$$\text{(c)} \quad G_L = \frac{1 + \phi \eta V_f}{1 - \eta V_f} G_m \tag{26}$$

$$\eta = \left(\frac{G_f}{G_m} - 1\right) \Big/ \left(\frac{G_f}{G_m} + \phi\right)$$

$$\phi = \left(\frac{a}{b}\right)^{\sqrt{3}} \text{ for rectangular fiber}$$

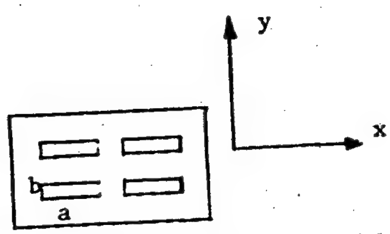

$G_L = G_{XZ}$

$\phi = 1$ for circular fiber

Source: Reference 2

(d) $$G_L = \frac{2G_f - (G_f - G_m)\,V_m}{2G_m + (G_f - G_m)\,V_m}\,G_m \tag{27}$$

Source: Reference 10

(e) $$G_L \text{ (lower bound)} = G_m + \frac{V_f}{\dfrac{1}{G_f - G_m} + \dfrac{V_m}{2G_m}} \tag{28}$$

Source: Reference 11

(f) $$G_L \text{ (upper bound)} = G_f + \frac{V_m}{\dfrac{1}{G_m - G_f} + \dfrac{V_f}{2G_f}} \tag{29}$$

Source: Reference 11

(g) $$G_L = \frac{G_m}{2}\left[\frac{4 - \pi + \pi\phi}{4} + \frac{\phi}{\phi(4 - \pi) + \pi}\right] \tag{30}$$

$$\phi = \frac{G_f\ (\pi + 4V_f) + (G_m\ \pi - 4V_f)}{G_f\ (\pi - 4V_f) + (G_m\ \pi + 4V_f)}$$

Source: Reference 23

APPENDIX II

Whitney[25] has investigated the influence of twist on graphite fibers in an epoxy matrix. He derived an equation for the reduction of the longitudinal elastic Young's modulus for graphite as a function of the geometry of the fibers. This equation is directly applicable in estimating how twisting affects a superconducting wire.

If the initial and reduced moduli are E_I and E_R, respectively, then their ratio can be expressed as:[25]

$$\frac{E_R}{E_I} = \frac{1}{1 + 4\pi^2 N_o^2 R^2} ,$$

where N_o is the number of twists per centimeter and R is the radius of the fiber in centimeters.

For the superconducting wire analyzed in this report,

$$N_o = .132 \text{ cm}^{-1}$$

$$R = 3.17 \times 10^{-3} \text{cm},$$

which yields

$$\frac{1}{1 + 4\pi^2 N_o^2 R^2} = \frac{1}{1 + 6.87 \times 10^{-6}} \approx 1.$$

Clearly, the effect of twist for this superconducting wire can be neglected.

APPENDIX III

```
FIBERC
VIA

LPTSPL Version 6(34404)  Running on EPL000
 *START* User GRAY  [200,2304] Job  FIBERC Seq. 6417 Date 17-May-76 16:03:00 Monitor ORNL-USC KI-10 NET 602 *START*
Request created: 17-May-76  16:04:07
File: DSKB0:FIBERC.VIA[200,2304] Created: 02-Apr-76 10:40:00 <157>  Printed: 17-May-76 16:03:17
QUEUE Switches:  /PRINT:ARROW /FILE:ASCII /COPIES:1 /SPACING:1 /LIMIT:34 /FORMS:NORMAL
File will be RENAMEd to <057> protection
```

```
C
C  PROGRAM FIBERC.V1A
C
C  LAST UPDATE: 1APR76
C
C  AUTHOR:  W. J. GRAY
C           P. O. BOX Y 9204-1
C           OAK RIDGE NATIONAL LABORATORY
C           OAK RIDGE, TN. 37830
C
C  LANGUAGE: DECSYSTEM-10, FORTRAN-10
C
C  SUBROUTINES REQUIRED:
C
C     MINV - STANDARD IBM SCIENTIFIC SUBROUTINE PACKAGE.
C
      IMPLICIT REAL (K)
      REAL NUF,NUM
      DIMENSION U(6,6),RES(6),L(6),M(6),H(6)
      DIMENSION UINV(6,6)
      DIMENSION ELEM(2),XNULT(2),GLGM(7),GTGM(5),
     1 KTKM(4),ETEM(5)
      DATA PI/3.1415926/
      DATA IORED,IOWRT/5,5/
C
C  BEGIN PROGRAM    FIBERC.V1A
C
C
C  QUERY THE USER FOR THE MATERIAL PROPERTIES
      WRITE(IOWRT, 11)
11    FORMAT(//' FIBERC.V1A  DOCUMENTED IN ORNL/TM-5331'//
     1 ' INPUT IN THE FOLLOWING ORDER:'/
     2 ' EF(FIBER YOUNGS MODULUS)'/
     3 ' EM(MATRIX YOUNGS MODULUS)'/
     4 ' NUF(FIBER POISSONS RATIO)'/
     5 ' NUM(MATRIX POISSON RATIO)'/
     6 ' VF(FIBER VOLUME FRACTION)'//
     7 ' ORDER IS EF,EM,NUF,NUM,VF FORMAT(5F)'/
     8 ' REMEMBER A SPACE DELIMITS THE INPUT VARIABLES'/)
      READ(IORED,10)EF,EM,NUF,NUM,VF
10    FORMAT(5F)
909   CONTINUE
C
C  CALCULATE THE SHEAR MODULII
      GF=EF/(2.*(1.+NUF))
      GM=EM/(2.*(1.+NUM))
C  CALCULATE THE MATRIX VOLUME FRACTION
      VM=1.-VF
C
C  CALCULATE THE BULK MODULII
      KF=EF/(3.*(1.-2.*NUF))
      KM=EM/(3.*(1.-2.*NUM))
C
C  CALCULATE THE FIBER-MATRIX RATIOS.
      GMGF=GM/GF
      GFGM=GF/GM
      EFEM=EF/EM
      EMEF=EM/EF
      GMEM=GM/EM
      KMGM=KM/GM
      KFGF=KF/GF
```

```
      KFGM=KF/GM
C ECHO INPUT DATA
      WRITE(IOWRT,29) EF,EM,NUF,NUM,VF,GF,GM,EFEM,KF,KM,GFGM
29    FORMAT(//' INPUT DATA'//,
     1' EF = ',T10,1PE11.4,/,
     2' EM = ',T10,1PE11.4,/,
     3' NUF = ',T10,1PE11.4,/,
     4' NUM = ',T10,1PE11.4,/,
     5' VF = ',T10,1PE11.4,/,
     6' GF = ',T10,1PE11.4,/,
     7' GM = ',T10,1PE11.4,/,
     8' EF/EM = ',T10,1PE11.4,/,
     9' KF = ',T10,1PE11.4,/,
     .' KM = ',T10,1PE11.4,/,' GF/GM = ',T10,1PE11.4)
C
C  THE EQUATION NUMBERS GIVEN IN THE REST OF THIS CODE REFER
C  TO ORNL/TM-5331
C
C  CALCULATE THE LONGITUDINAL YOUNG'S MODULUS
C
C  EQUATION 10
      ELEM(1)=VF*EFEM+VM
C  EQUATION 11
      IF(VM.NE.0.0) GO TO 21
      ALPHA=1.
      GO TO 20
21    CONTINUE
      F1=(NUM*VF*EFEM+NUF*VM)/(NUF*VF*EFEM+NUF*VM)
      F2=NUF*F1/NUM
      D1=1.-NUF
      D2=(1.+VF)/VM+NUM
      D3=2.*NUF*NUF
      D4=2.*NUM*NUM*VF/VM
      ALPHA=D1-D3*F1+EFEM*(D2-D4*F2)
      ALPHA=ALPHA/(D1-D3+EFEM*(D2-D4))
20    ELEM(2)=ELEM(1)*ALPHA
      WRITE(IOWRT,25)
25    FORMAT(//,' LONGITUDINAL MODULUS'/)
C  OUTPUT DATA ON DATA FILE
      DO 801 J=1,2
801   ELEM(J)=ELEM(J)*EM
      DO 30 J=1,2
      JJ=J+9
      WRITE(IOWRT,24) JJ,ELEM(J)
30    CONTINUE
24    FORMAT(1X,'EQU. ',I2,4X,1PE11.4)
C
C  CALCULATE THE MAJOR POISSON RATIO
C
C  EQUATION 12
      XL1=2.*NUF*(1.-NUM*NUM)*VF+NUM*(1.+NUM)*VM
      XL2=VF*(1.-NUF-2.*NUF*NUF)
      XL3=2.*(1.-NUM*NUM)*VF+(1.+NUM)*VM
      XNULTA=VF*EFEM*XL1+VM*NUM*XL2
      XNULT(1)=XNULTA/(VF*EFEM*XL3+VM*XL2)
C
C  EQUATION 13
      XNULT(2)=VF*NUF+VM*NUM
      WRITE(IOWRT, 225)
225   FORMAT(//,' MAJOR POISSONS RATIO'/)
```

```
C  OUTPUT DATA ON DATA FILE
      DO 31 J=1.2
      JJ=J+11
      WRITE(IOWRT.24) JJ.XNULT(J)
31    CONTINUE
C
C  CALCULATE THE TRANSVERSE YOUNG'S MODULUS
C
C
C  EQUATION 14
      ETEM(1)=1./(VM+EMEF*VF)
C
C  EQUATION 15
      ETA=(EFEM-1.)/(EFEM+2.)
      ETEM(2)=(1.+2.*ETA*VF)/(1.-ETA*VF)
C
C  EQUATION 16
      XMF=EFEM/(2.*(1.-NUF))
      XMM=1./(2.*(1.-NUM))
      PART=2.*(1.-NUF+(NUF-NUM)*VM)
      PART=PART*(XMF*(2.*XMM+GMEM)-GMEM*(XMF-XMM)*VM)
      ETEM(3)=PART/(2.*XMM+GMEM+2.*(XMF-XMM)*VM)
C
C  EQUATION 17
      ALPHA=2.*(EMEF-1.)
C
C  CHECK FOR A POSITIVE RADICAL FOR SQRT.
      IF(1.-ALPHA*ALPHA*VF/PI.LE.0.) GO TO 160
      XNMR=SQRT(1.-ALPHA*ALPHA*VF/PI)
      TANSTF=ATAN2(XNMR.(1.+SQRT(ALPHA*ALPHA*VF/PI)))
      SQ=4./SQRT(1.-ALPHA*ALFHA*VF/PI)
      ETEM(4)=1.-2.*SQRT(VF/PI)+(PI-SQ*TANSTF)/ALPHA
      GO TO 161
160   CONTINUE
      ETEM(4)=-1.
161   CONTINUE
C
C  EQUATION 18
      SQ=(EFEM*NUM-NUF)**2*VF/EF
      ETEM(5)=VM/EM+VF/EF-SQ/(VF*EF/VM/EM+1.)
      ETEM(5)=1./(ETEM(5)*EM)
      WRITE(IOWRT. 625)
625   FORMAT(//.' TRANSVERSE YOUNGS MODULUS'/)
C  OUTPUT DATA ON DATA FILE
      EHG=AMAX1(EF.EM)
      ELW=AMIN1(EF.EM)
      DO 805 J=1.5
805   ETEM(J)=ETEM(J)*EM
      DO 32 J=1.5
      JJ=J+13
      IF(ETEM(J).GT.EHG.OR.ETEM(J).LT.ELW) GO TO 82
      WRITE(IOWRT.24) JJ.ETEM(J)
      GO TO 32
82    WRITE(IOWRT.83) JJ
83    FORMAT(' EQU. '.I2.' NOT APPLICABLE')
32    CONTINUE
C
C  CALCULATE THE TRANSVERSE SHEAR MODULUS
C
C
C  EQUATION 19
C
```

```
C  BEGIN TO SET UP THE COEFFICIENT MATRIX
      U(1,1)=1.
      U(2,1)=0.
      U(3,1)=1.
      U(4,1)=0.
      U(5,1)=1.
      U(6,1)=0.
      U(3,2)=1.
      U(3,3)=1.
      U(4,3)=-2.
      U(5,3)=-3.
      U(6,3)=2.
      U(3,4)=1.
      U(1,5)=0.
      U(2,5)=0.
      U(3,5)=-1.
      U(4,5)=0.
      U(6,5)=0.
      U(1,6)=0.
      U(2,6)=0.
      U(3,6)=-1.
      U(1,2)=1./VF
      U(4,2)=-(3.-4.*NUM)/(3.-2.*NUM)
      U(2,2)=U(4,2)/VF
      U(6,2)=-1./(3.-2.*NUM)
      U(5,2)=-3.*U(6,2)
      U(1,3)=VF*VF
      U(2,3)=-2.*U(1,3)
      U(1,4)=VF
      U(4,4)=1./(1.-2.*NUM)
      U(2,4)=VF*U(4,4)
      U(5,4)=U(4,4)
      U(6,4)=-U(4,4)
      U(5,5)=-GFGM
      U(4,6)=(3.-4.*NUF)/(3.-2.*NUF)
      U(6,6)=GFGM/(3.-2.*NUF)
      U(5,6)=-3.*U(6,6)
C
C  STORE THE COEFFICIENT MATRIX INTO UINV
      DO 71 IH=1,6
      DO 71 JH=1,6
71    UINV(IH,JH)=U(IH,JH)
C
C  FORMULATE RIGHT HAND SIDE
      A(1)=1.
      A(2)=0.
      A(3)=0.
      A(4)=0.
      A(5)=0.
      A(6)=0.
C
C  INVERT THE COEFFICIENT MATRIX.  SUBROUTINE MINV IS THE STANDARD
C  IBM SCIENTIFIC SUBROUTINE MATRIX INVERTER.
      CALL MINV(UINV,6,D,L,M)
C
C  OBTAIN THE SOLUTION VECTOR
      DO 69 MK=1,6
      RES(MK)=0.
      DO 69 ML=1,6
69    RES(MK)=A(ML)*UINV(MK,ML)+RES(MK)
```

```
      GTGM(1)=1.-2.*(1.-NUM)*VF*RES(4)/(1.-2.*NUM)
C
C EQUATION 28
C
C BEGIN TO SET UP THE COEFFICIENT MATRIX
      U(1,1)=1.
      U(2,1)=0.
      U(3,1)=1.
      U(4,1)=0.
      U(5,1)=1.
      U(6,1)=0.
      U(1,2)=1.
      U(1,3)=1.
      U(2,3)=-2.
      U(3,3)=-3.
      U(4,3)=2.
      U(1,4)=1.
      U(1,5)=-1.
      U(2,5)=0.
      U(4,5)=0.
      U(5,5)=0.
      U(6,5)=0.
      U(1,6)=-1.
      U(5,6)=0.
      U(6,6)=0.
      U(4,2)=-1./(3.-2.*NUM)
      U(3,2)=-3.*U(4,2)
      U(2,2)=(3.-4.*NUM)*U(4,2)
      U(5,2)=U(3,2)/VF
      U(6,2)=U(4,2)/VF
      U(5,3)=-3.*VF*VF
      U(6,3)=2.*VF*VF
      U(2,4)=1./(1.-2.*NUM)
      U(3,4)=U(2,4)
      U(4,4)=-U(2,4)
      U(5,4)=VF*U(2,4)
      U(6,4)=-U(5,4)
      U(3,5)=-GFGM
      U(2,6)=(3.-4.*NUF)/(3.-2.*NUF)
      U(4,6)=GFGM/(3.-2.*NUF)
      U(3,6)=-3.*U(4,6)
C
C STORE THE COEFFICIENT MATRIX INTO UINV.
      DO 81 IH=1,6
      DO 81 JH=1,6
81    UINV(IH,JH)=U(IH,JH)
C
C FORMULATE THE RIGHT HAND SIDE.
      A(1)=0.
      A(2)=0.
      A(3)=0.
      A(4)=0.
      A(5)=1.
      A(6)=0.
C
C INVERT THE MATRIX.
      CALL MINV(UINV,6,D,L,M)
C
C OBTAIN THE SOLUTION VECTOR.
      DO 89 MK=1,6
```

```
      RES(MK)=0.
      DO 89 ML=1.6
89    RES(MK)=A(ML)*UINV(MK.ML)+RES(MK)
      GTGM(2)=1./(1.+2.*(1.-NUM)/(1.-2.*NUM)*VF*RES(4))
C
C EQUATION 21
      KMGM1=(KMGM+1.)*VF*2.
      GFGM1=(GFGM+1.)*VM*KMGM
      GTGMC=GFGM*KMGM1+2.*GFGM*VM+GFGM1
      GTGM(3)=GTGMC/(KMGM1+2.*GFGM*VM+GFGM1)
C
C EQUATION 22
      GTGM(4)=1.+VF/(1./(GFGM-1.)+(KMGM+2.)*VM/(2.*(KMGM+1.)))
C
C EQUATION 23
       FRAC=((KFGF+2.)*VF/2./(KFGM+GFGM)+1./(1.-GFGM))
100   GTGM(5)=GFGM+VM/FRAC
      WRITE(IOWRT. 425)
425   FORMAT(//.' TRANSVERSE SHEAR MODULUS'/)
C OUTPUT DATA ON DATA FILE
      DO 883 J=1.5
883   GTGM(J)=GTGM(J)*GM
      DO 33 J=1.5
      JJ=J+10
      WRITE(IOWRT.24) JJ.GTGM(J)
33    CONTINUE
C
C CALCULATE THE MINOR POISSON RATIO USING THE RULE OF MIXTURES
C TRANSVERSE YOUNG'S MODULUS AND EACH OF THE PREVIOUSLY CALCULATED
C TRANSVERSE SHEAR MODULII.
C
      E22=ETEM(1)
      WRITE(IOWRT.79)
      DO 75 J=1.5
      JJ=J+10
C
C EQUATION 1
      POI23=(E22/(2.*GTGM(J)))-1.
      IF(POI23.LT.0.0.OR.POI23.GT.0.5) GO TO 76
      WRITE(IOWRT.77) JJ.POI23
      GO TO 75
76    WRITE(IOWRT.78) JJ
75    CONTINUE
77    FORMAT(' EQU. 1 USING EQU. '.I2.4X.1PE11.4)
78    FORMAT(' EQU. 1 USING EQU. '.I2.' NOT APPLICABLE')
79    FORMAT(//.' MINOR POISSONS RATIO'/)
C
C CALCULATE THE LONGITUDINAL SHEAR MODULUS
C
C EQUATION 24
      GLGM(1)=(GFGM*(1.+VF)+VM)/(GFGM*VM+1.+VF)
C
C EQUATION 25
      GLGM(2)=1./(VM+GMGF*VF)
C
C EQUATION 26
      ETA=VF*(GFGM-1.)/(GFGM+1.)
      GLGM(3)=(1.+ETA)/(1.-ETA)
C
C EQUATION 27
```

```
      GLGMD=2.*GFGM-(GFGM-1.)*VM
      GLGM(4)=GLGMD/(2.+(GFGM-1.)*VM)
C
C  EQUATION 28
      FRAC=1./(GFGM-1.)
      GLGM(5)=1.+VF/(FRAC+VM/2.)
C
C  EQUATION 29
      FRAC=1./(1.-GFGM)+VF/(2.*GFGM)
      GLGM(6)=GFGM+VM/FRAC
C
C  EQUATION 30
      ALPHA=GFGM*(4.*VF+PI)+PI-4.*VF
      ALPHA=ALPHA/(GFGM*(PI-4.*VF)+PI+4.*VF)
      GLGM(7)=.5*((4.-PI+PI*ALPHA)/4.+4.*ALPHA/(ALPHA*(4.-PI)+PI))
      WRITE(IOWRT, 325)
325   FORMAT(//,' LONGITUDINAL SHEAR MODULUS'/)
C  OUTPUT DATA ON DATA FILE
      GHG=AMAX1(GF,GM)
      GLW=AMIN1(GF,GM)
      DO 882 J=1,7
882   GLGM(J)=GLGM(J)*GM
      DO 34 J=1,7
      JJ=J+23
      IF(GLGM(J).GT.GHG.OR.GLGM(J).LT.GLW) GO TO 85
      WRITE(IOWRT,24) JJ,GLGM(J)
      GO TO 34
85    WRITE(IOWRT,83) JJ
34    CONTINUE
C
C  MORE DATA
      WRITE(IOWRT, 998)
998   FORMAT(//' MORE DATA?'/
     1 ' INPUT EF,EM,NUF,NUM,VF FORMAT(5F)'/
     2 ' NEGATIVE EF STOPS THE PROGRAM')
      READ(IORED,10)EF,EM,NUF,NUM,VF
      IF(EF.GT.0.) GO TO 989
      STOP
      END
```

ACKNOWLEDGMENTS

The authors wish to thank S. E. Bolt for his assistance with the experimental aspect of this paper and C. J. Long and W.C.T. Stoddart for their useful comments during the preparation of this manuscript. We also wish to thank K. E. Rothe for her assistance with the computer program listed in Appendix III.

FIGURE CAPTIONS

Fig. 1. Direction of loading for the determination of the longitudinal Young's modulus and the major Poisson's ratio.

Fig. 2. σ_1 vs ε_1 diagram for Kryo-210 superconductor.

Fig. 3. Normalized plot of the longitudinal Young's Modulus versus volume fraction of the fiber (NbTi): In this graph, as well as the other normalized comparison graphs, the legend refers to the theoretical equations presented in Appendix I.

Fig. 4. ε_2 vs ε_1 diagram for Kryo-210 superconductor.

Fig. 5. Normalized plot of the major Poisson's ratio vs volume fraction of the fiber (NbTi).

Fig. 6. Direction of loading for the determination of the transverse Young's Modulus and the minor Poisson's ratio.

Fig. 7. σ_2 vs ε_2 diagram for Kryo-210 superconductor.

Fig. 8. Normalized plot of the transverse Young's Modulus versus volume fraction of the fiber (NbTi).

Fig. 9. ε_3 vs ε_2 diagram for Kryo-210 superconductor.

Fig. 10. Normalized plot of G_{23} vs the volume fraction of the fiber (NbTi).

Fig. 11. Coordinate system for the determination of the longitudinal shear modulus.

Fig. 12. Normalized plot of the longitudinal shear modulus vs volume fraction of the fiber (NbTi).

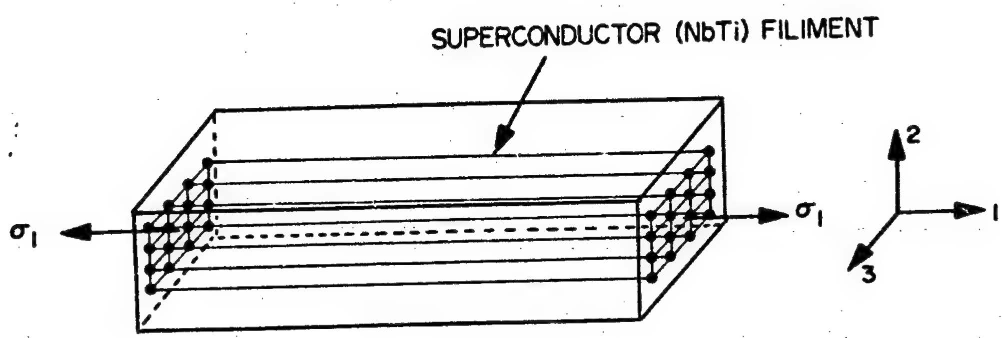

Figure 1

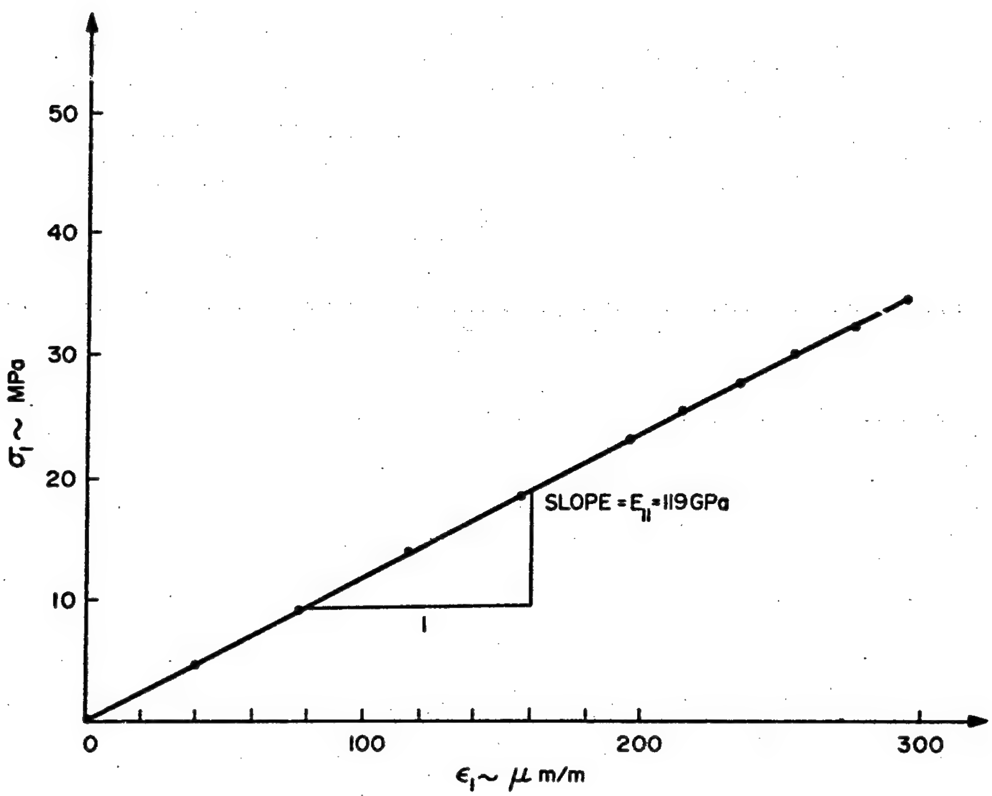
50
40
30
20
10
0
100
200
300
$\sigma_1 \sim$ MPa
$\epsilon_1 \sim \mu$ m/m
SLOPE = E_{11} = 119 GPa
1

Figure 2

ORNL DWG. 75-16576

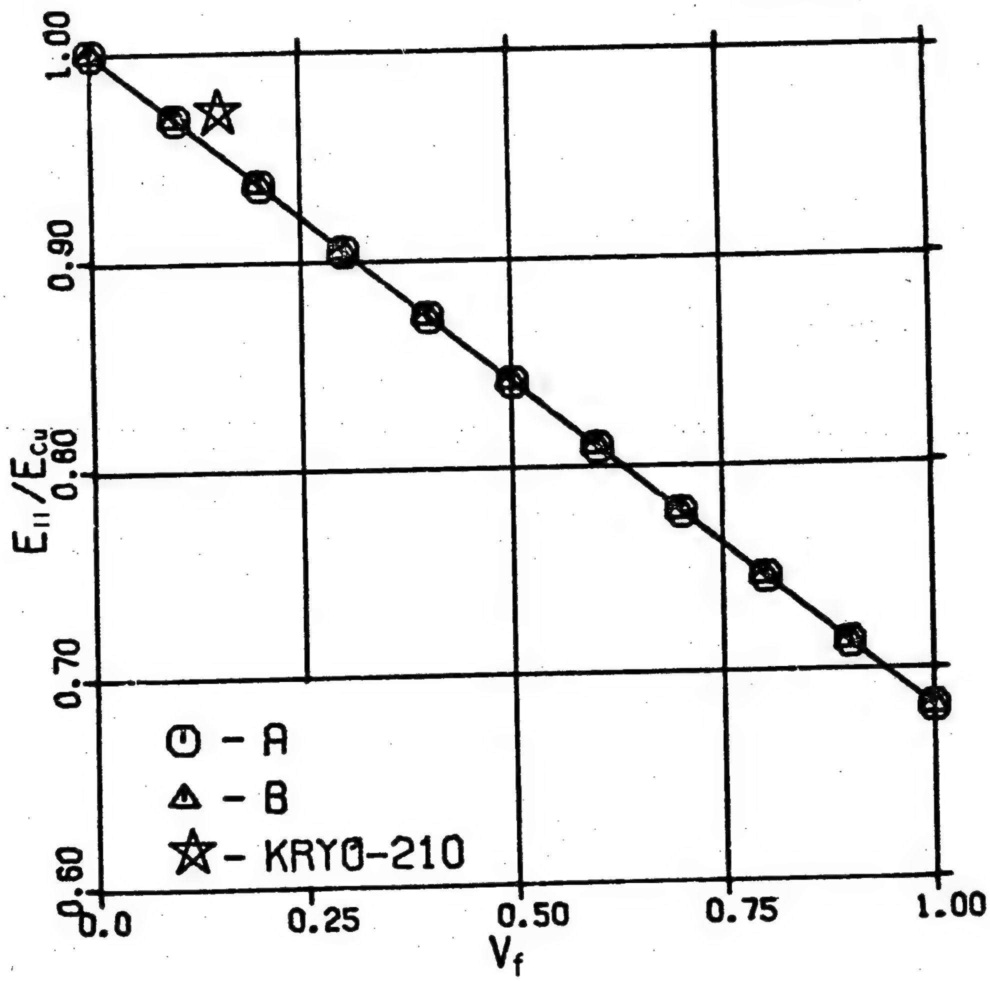

Figure 3

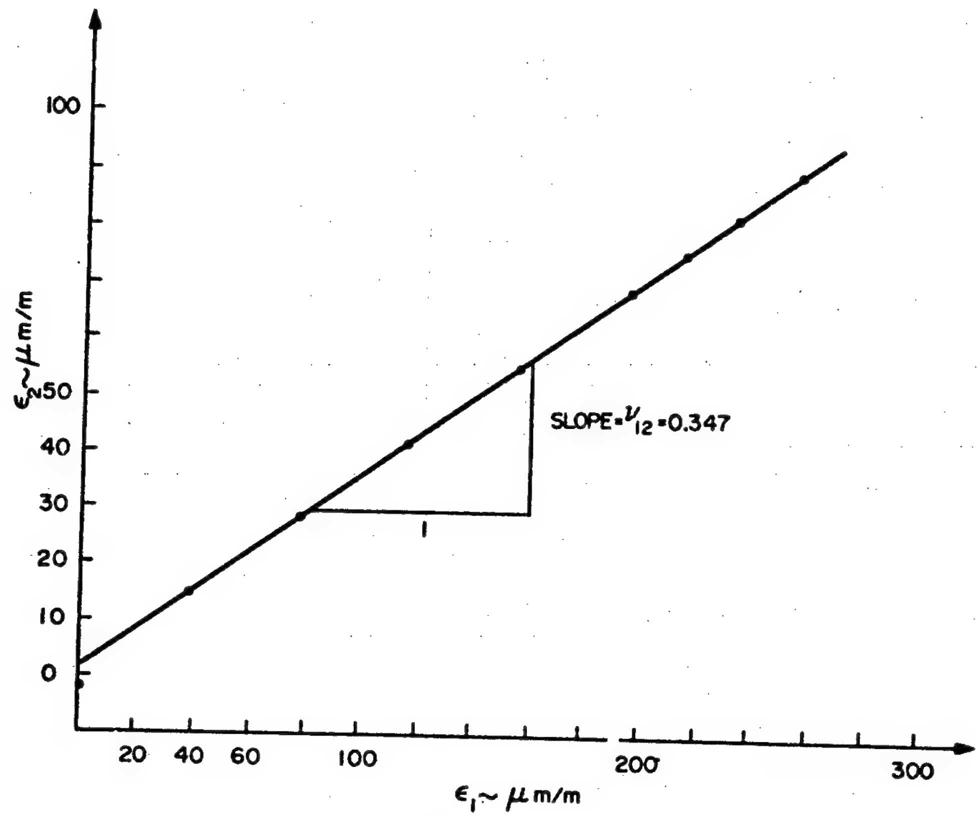
100
50
40
30
20
10
0
$\epsilon_2 \sim \mu$m/m
SLOPE = ν_{12} = 0.347
1
20 40 60 100 200 300
$\epsilon_1 \sim \mu$m/m

Figure 4

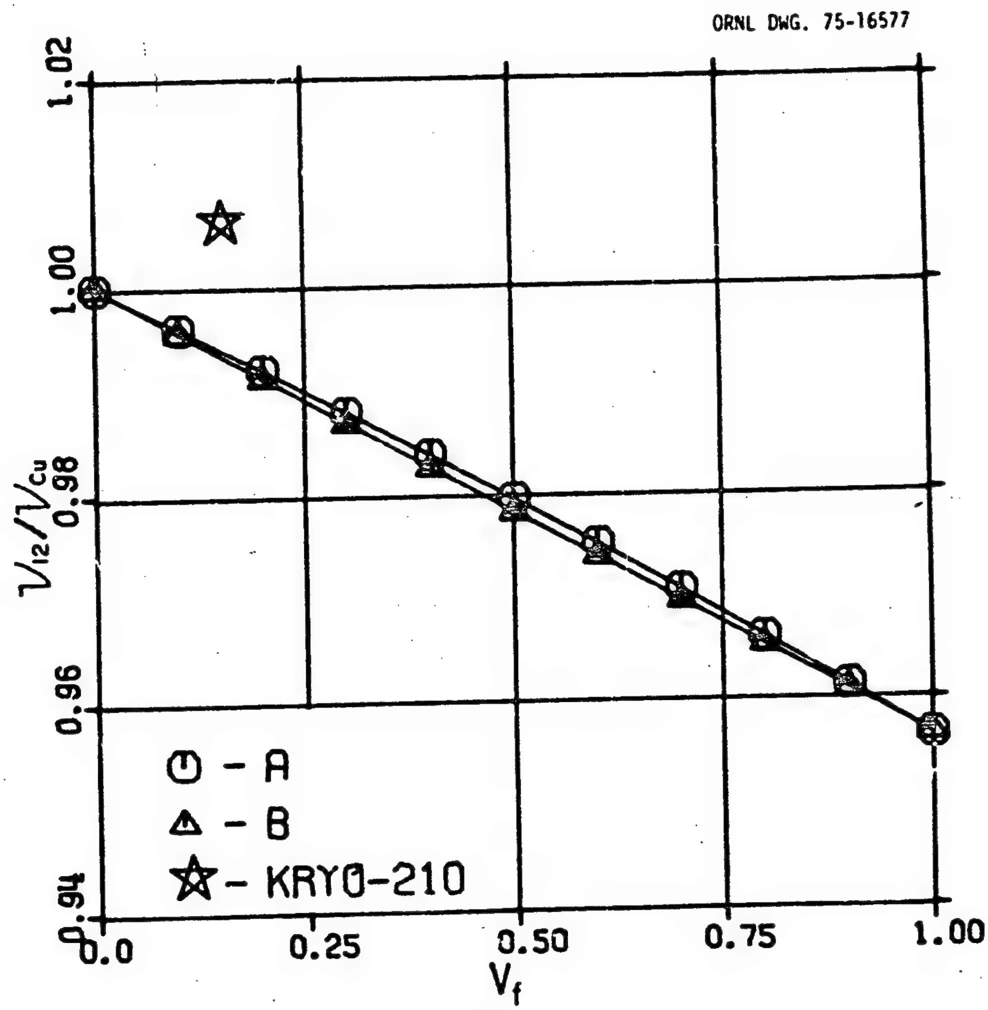
ORNL DWG. 75-16577
1.02
1.00
0.98
0.96
0.94
ν_{12}/ν_{Cu}
0.0
0.25
0.50
0.75
1.00
V_f
- A
- B
- KRYO-210

Figure 5

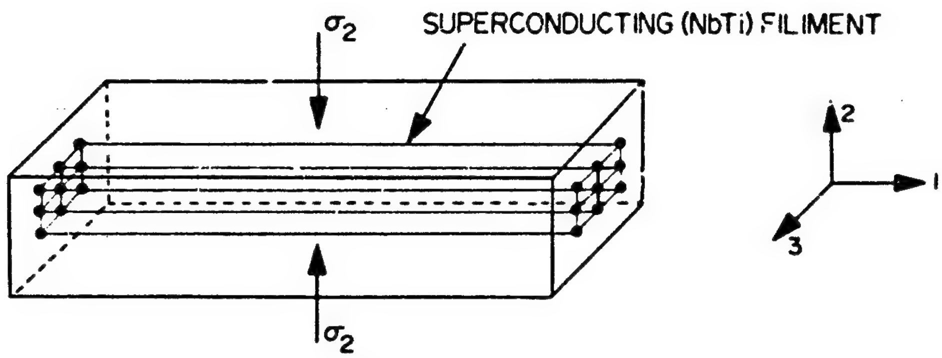

Figure 6

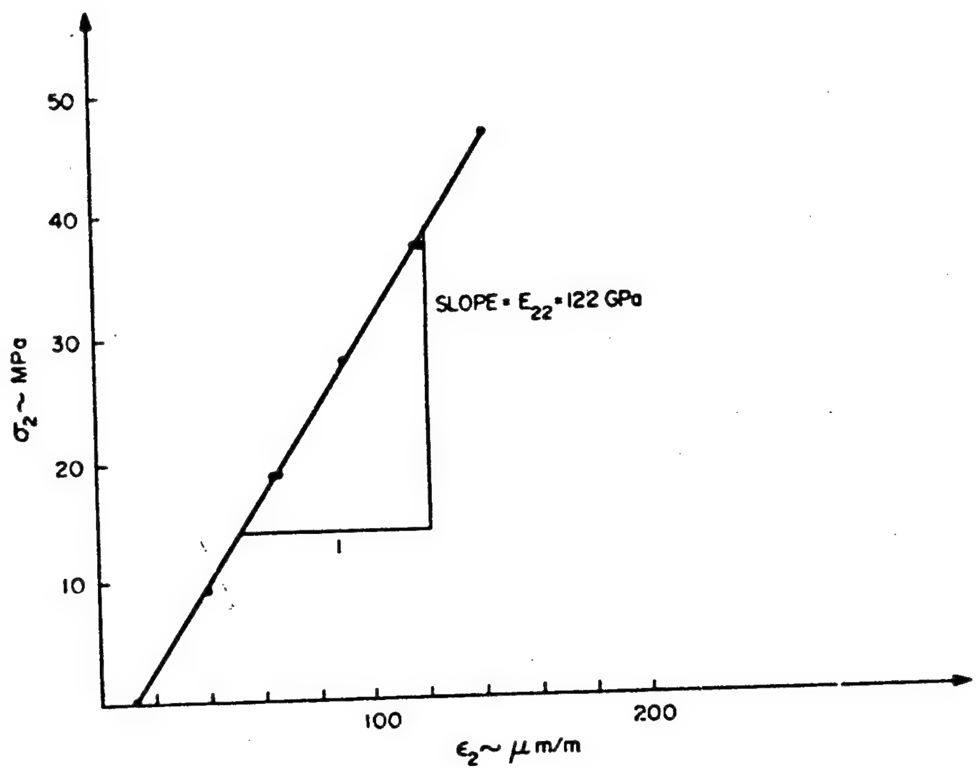
50
40
30
20
10
σ_2 ~ MPa
SLOPE = E_{22} = 122 GPa
1
100
200
ϵ_2 ~ μm/m

Figure 7

ORNL DWG. 75-16575

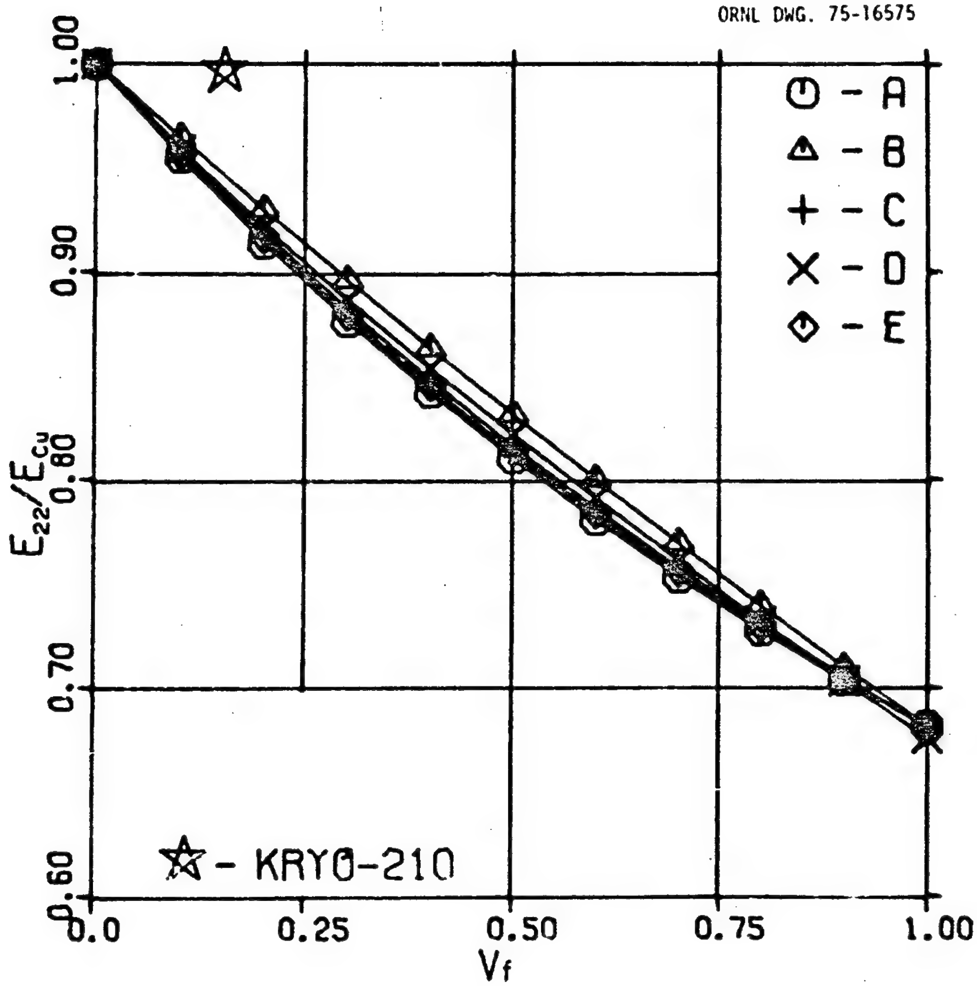

Figure 8

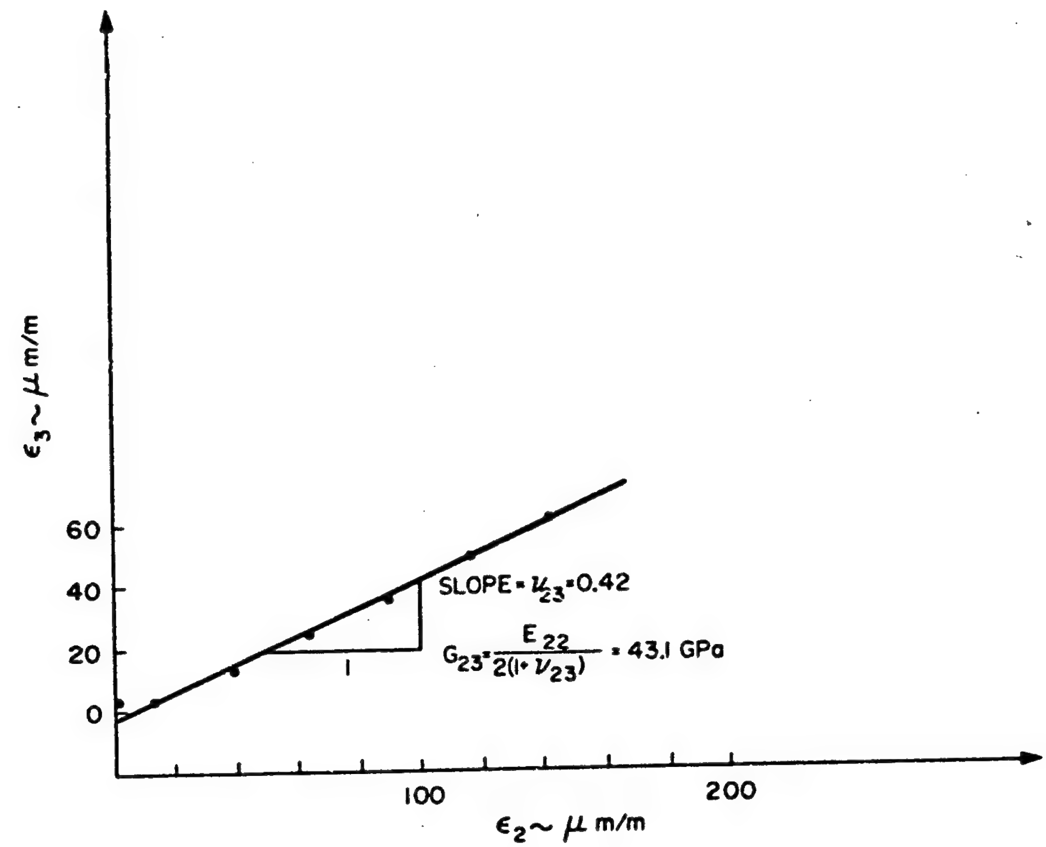

$\epsilon_3 \sim \mu$ m/m
60
40
20
0
SLOPE = ν_{23} = 0.42
1
$G_{23} = \frac{E_{22}}{2(1+\nu_{23})}$ = 43.1 GPa
100
200
$\epsilon_2 \sim \mu$ m/m

Figure 9

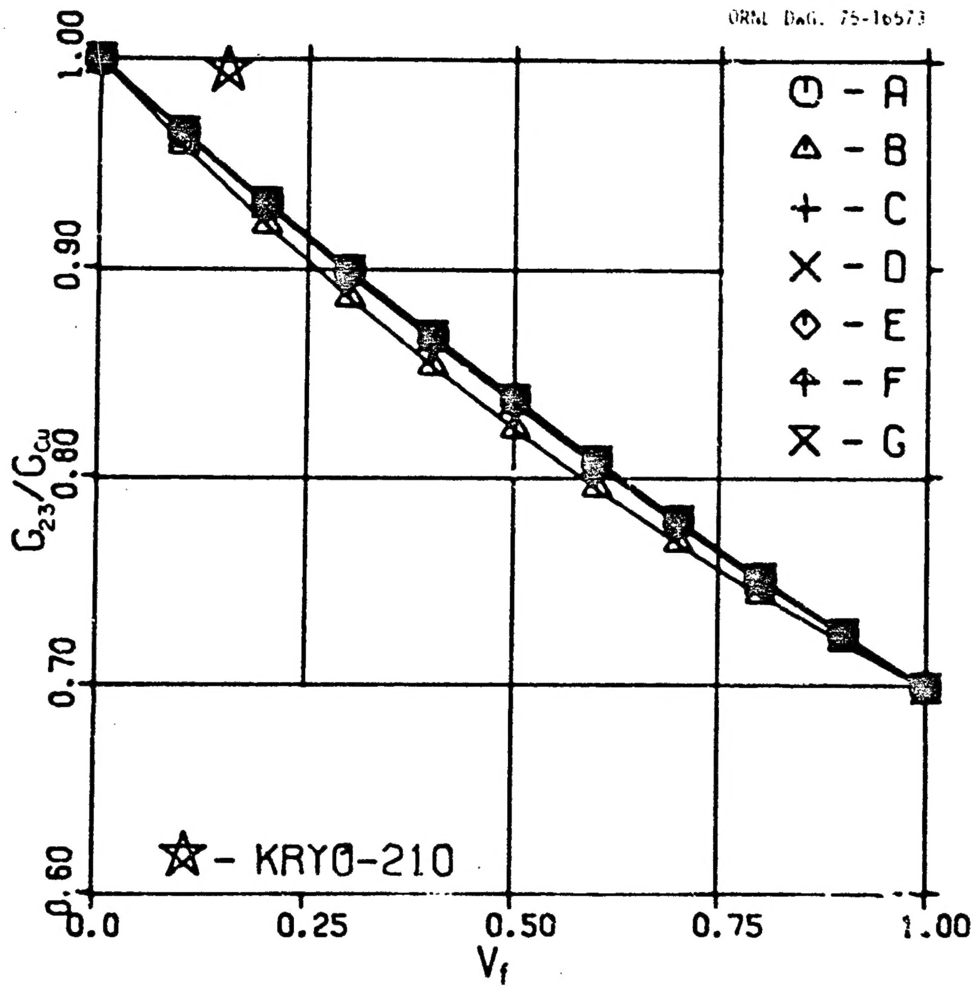
ORNL DWG. 75-16573
1.00
0.90
0.80
0.70
0.60
G_{23}/G_{cu}
0.0
0.25
0.50
0.75
1.00
V_f
- A
- B
- C
- D
- E
- F
- G
- KRYO-210

Figure 10

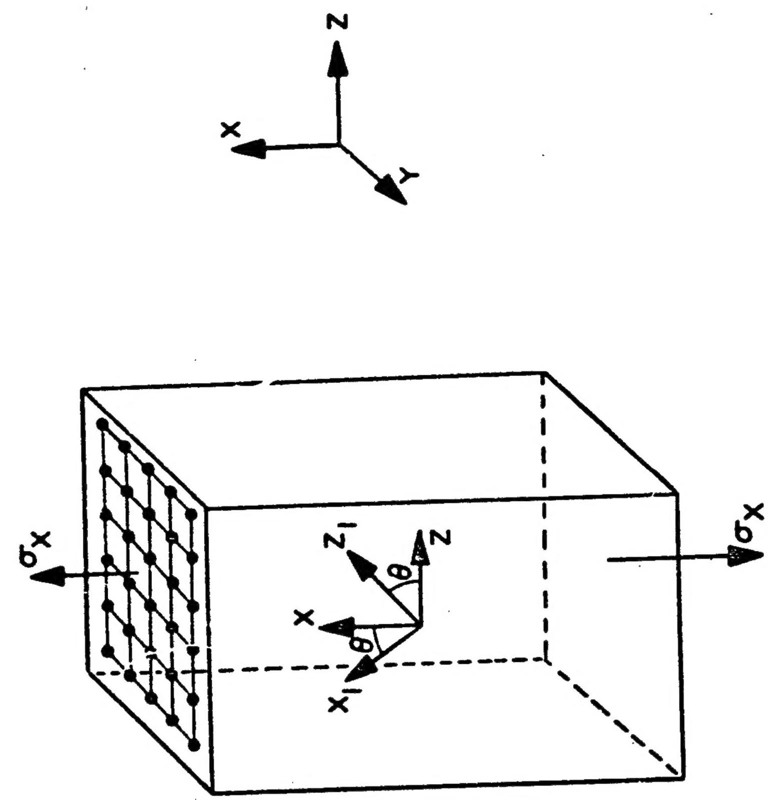

Figure 11

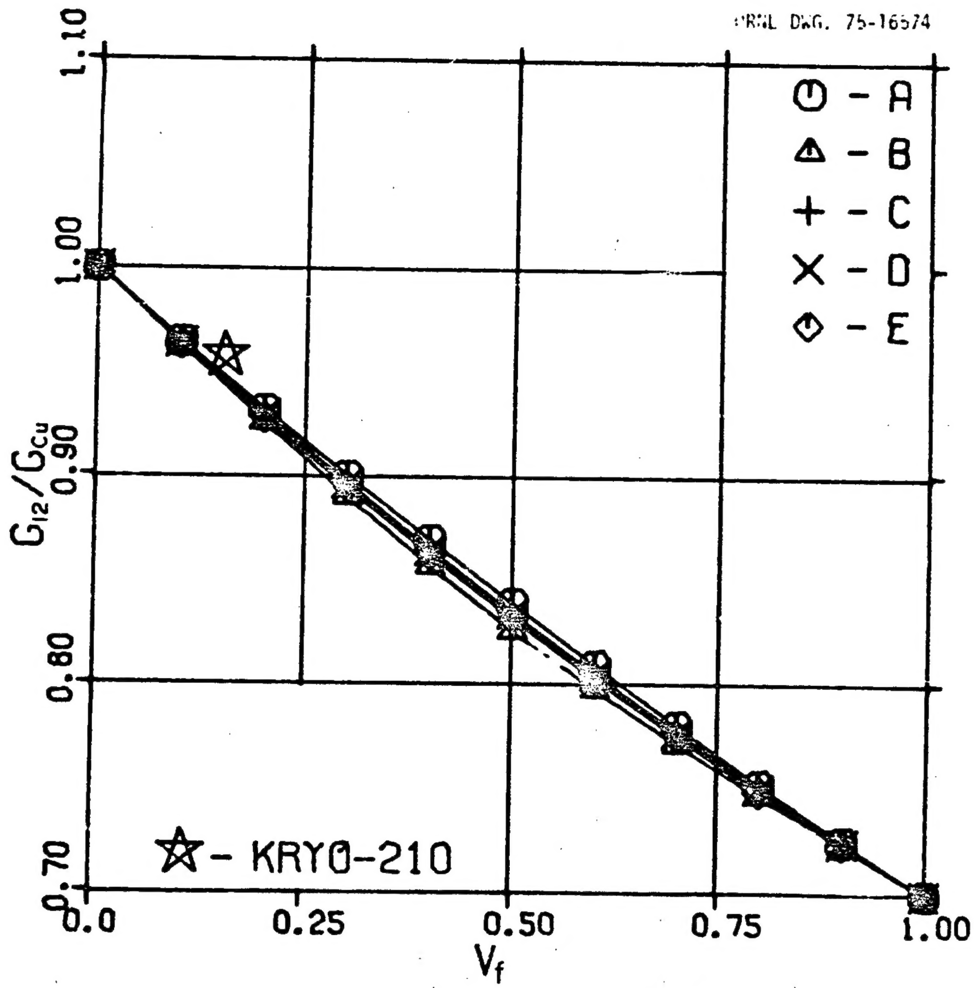
ORNL DWG. 75-16574
1.10
1.00
0.90
0.80
0.70
G12/Gcu
0.0
0.25
0.50
0.75
1.00
Vf
- A
- B
- C
- D
- E
- KRYO-210

Figure 12

END

DATE FILMED

9 / 23 /76